JOURNAL OF VIROLOGY, Mar. 2011, p. 2037–2049 Vol. 85, No. 5
0022-538X/11/$12.00 doi:10.1128/JVI.02236-10

Orf Virus *ORFV121* Encodes a Novel Inhibitor of NF-κB That Contributes to Virus Virulence▽

D. G. Diel,[1,2]† S. Luo,[1]† G. Delhon,[3]† Y. Peng,[1,4] E. F. Flores,[2] and D. L. Rock[1]*

Department of Pathobiology, College of Veterinary Medicine, University of Illinois, Urbana, Illinois[1]; Programa de Pós-graduação em Medicina Veterinária, Setor de Virologia, Departamento de Medicina Veterinária Preventiva, Centro de Ciências Rurais, Universidade Federal de Santa Maria, Rio Grande do Sul, Brazil[2]; Department of Veterinary and Biomedical Sciences and Nebraska Center for Virology, University of Nebraska–Lincoln, Lincoln, Nebraska[3]; and Department of Laboratory Medicine, Zhujiang Hospital, Southern Medical University, Guangdong, China[4]

Received 25 October 2010/Accepted 7 December 2010

Orf virus (ORFV), the type member of the genus *Parapoxvirus* of the *Poxviridae*, has evolved novel strategies (proteins and/or mechanisms of action) to modulate host cell responses regulated by the nuclear factor-κB (NF-κB) signaling pathway. Here, we present data indicating that ORFV *ORFV121*, a gene unique to parapoxviruses, encodes a novel viral NF-κB inhibitor that binds to and inhibits the phosphorylation and nuclear translocation of NF-κB-p65. The infection of cells with an *ORFV121* deletion mutant virus (OV-IA82Δ121) resulted in increased NF-κB-mediated gene transcription, and the expression of ORFV121 in cell cultures significantly suppressed NF-κB-regulated reporter gene expression. ORFV ORFV121 physically interacts with NF-κB-p65 in the cell cytoplasm, thus providing a mechanism for the inhibition of NF-κB-p65 phosphorylation and nuclear translocation. Notably, the deletion of *ORFV121* from the viral genome markedly decreased ORFV virulence and disease pathogenesis in sheep, indicating that ORFV121 is a virulence determinant for ORFV in the natural host.

Orf, also known as contagious ecthyma or scabby mouth, is a nonsystemic, ubiquitous disease of sheep and goats caused by orf virus (ORFV), the type member of the genus *Parapoxvirus* of the *Poxviridae* (31). The disease is characterized by inflammatory, often proliferative lesions affecting the skin of the lips, muzzle, nostrils, teats, and oral mucosa (20). Lesions, usually limited to areas surrounding the virus entry sites, evolve through stages of erythema, vesicles, pustules, and scabs (16). In the absence of secondary infections, lesions usually are resolved in 6 to 8 weeks; however, persistent infections have been reported (9, 18, 35). In spite of a vigorous and typical antiviral T-helper type 1 (Th1) immune response, immunity elicited by ORFV is short-lived, and animals can be repeatedly infected, although lesions are smaller and resolve sooner than those in primary infections (19, 52). Orf is a zoonotic disease, affecting humans in close contact with infected animals (15, 32, 43).

ORFV is an epitheliotropic virus, and no cell type other than keratinocytes, or their counterparts in the oral mucosa, has been shown to support ORFV replication *in vivo* (23, 27). Keratinocytes produce the protective stratum corneum of the epidermis and function as immune sentinels and instigators of cutaneous inflammation (39). These cells express several Toll-like receptors (TLRs) and receptors encoded by the nucleotide-binding domain leucine-rich repeat-containing (NLR) family members (reviewed in reference 36), which recognize pathogen-associated molecular patterns (PAMPs) and endogenous danger-associated molecular patterns (DAMPs), leading to the activation of proinflammatory signaling pathways, including the nuclear factor-kappa B (NF-κB) signaling pathway (36).

The NF-κB family of transcription factors NF-κB-p65 (RelA), RelB, c-Rel, NF-κB-p50/p105, and NF-κB-p52/p100 form homo- or heterodimers and bind to specific promoter DNA sequences to mediate the expression of a wide variety of cellular genes, including many involved in innate immunity, inflammation, cell proliferation and differentiation, and apoptosis (41, 44, 49). Various stimuli, including the proinflammatory cytokines tumor necrosis factor α (TNF-α) and interleukin 1 (IL-1), bacterial lipopolysaccharide (LPS), viruses, and viral products, lead to the phosphorylation of inhibitor-kappa B (IκB) proteins by IκB kinases (IKK complex), resulting in the proteasomal degradation of IκB and nuclear translocation of NF-κB subunits (25). NF-κB subunits are subject to extensive posttranslational modifications, including phosphorylation, acetylation, and methylation, which may facilitate their nuclear translocation or define their transcriptional functions (6, 40).

Recent studies using genetic mouse models to assess the function(s) of NF-κB signaling *in vivo* revealed a critical role for NF-κB in the maintenance of skin immune homeostasis (reviewed in reference 39). Notably, either continuous activation or continuous inhibition of the NF-κB signaling pathway in the epidermis resulted in enhanced skin inflammation (39). However, the mechanisms underlying these paradoxical effects of NF-κB in the skin remain poorly understood.

In addition to its role in the regulation of innate immune responses, the NF-κB signaling pathway also plays key func-

* Corresponding author. Mailing address: 2522 Veterinary Medicine Basic Science Building, University of Illinois, MC-002, 2001 S. Lincoln Ave., Urbana 61802, IL. Phone: (217) 333-2449. Fax: (217) 244-7421. E-mail: dlrock@illinois.edu.
† These authors contributed equally to this work.
▽ Published ahead of print on 22 December 2010.

tions in the maintenance of skin homeostasis by regulating keratinocyte proliferation, differentiation, and apoptosis (51). The inhibition of the NF-κB signaling pathway in transgenic murine and human epidermis has been shown to result in epidermal hyperplasia *in vivo*, while the overexpression of NF-κB-p50 and NF-κB-p65 subunits induced epidermal hypoplasia and growth inhibition (45). The deletion of the *IKK*α gene in transgenic murine epidermis led to epidermal hyperplasia and terminal differentiation defects in keratinocytes, indicating that IKKα functions as a switch for keratinocyte proliferation and differentiation (26). Although the importance of NF-κB signaling in skin homeostasis is well defined, the mechanisms underlying such regulation and the interplay among different components of the pathway remain elusive and await further experimentation.

Given the central role of NF-κB in the regulation of skin immune homeostasis and keratinocyte proliferation, differentiation, and apoptosis, it is not surprising that poxviruses have evolved various strategies to inhibit the NF-κB signaling pathway. Inhibitors of NF-κB have been identified in members of the genera *Orthopoxvirus*, *Leporipoxvirus*, *Yatapoxvirus*, *Molluscipoxvirus*, and *Parapoxvirus*, with selected viruses encoding multiple inhibitors (for a review, see reference 28). The type member of the *Poxviridae*, vaccinia virus (VACV), encodes at least seven NF-κB inhibitors (A52R, A46R, B14, K1L, N1L, M2L, and E3L), which target different steps leading to NF-κB activation, most often by preventing IKK complex activation (8, 13, 17, 21, 34, 46, 48). VACV proteins A46R and A52R, for example, associate with myeloid differentiation factor 88 (MyD88) and IRAK2 and TRAF6, respectively, disrupting the activation of the pathway through multiple TLRs (3, 21, 48). VACV protein B14 associates with IKK complex, inhibiting the phosphorylation of IKKβ (8). Molluscum contagiosum virus (MOCV) protein MC159 prevents the degradation of IκBβ, and MC160 induces the degradation of IKKα (33, 38).

The role of poxviral inhibitors of NF-κB during infection *in vivo* remains poorly understood. Pathogenesis studies using mutant viruses, with the deletion of selected NF-κB inhibitors, have shown a wide range of phenotypes *in vivo*, with individual gene deletions resulting in phenotypes from no effect (1, 8, 21, 48) to marked virus attenuation (4, 24, 30, 42).

With the exception of VACV E3L (ORFV020), the parapoxviruses lack homologues of NF-κB inhibitors encoded by other poxviruses, indicating that these viruses have evolved novel strategies to counteract the NF-κB signaling pathway. Recently, two novel inhibitors of NF-κB have been identified in the parapoxvirus ORFV, ORFV024 and ORFV002 (11, 12). ORFV024 was shown to inhibit the phosphorylation of IκB kinases, thus preventing the activation of the IKK complex (11), while ORFV002 encodes a nuclear NF-κB inhibitor that prevents the p300-mediated acetylation of the transactivating NF-κB subunit NF-κB-p65 (12).

Here, we present data indicating that ORFV *ORFV121*, a gene unique to parapoxviruses, encodes a novel viral NF-κB inhibitor that binds to and inhibits the phosphorylation and nuclear translocation of NF-κB-p65, a mechanism that is distinct from that of ORFV024- or ORFV002-mediated NF-κB inhibition. The deletion of ORFV121 from the viral genome markedly decreased ORFV virulence and disease severity in sheep, indicating that ORFV121 is a virulence determinant for ORFV in the natural host.

MATERIALS AND METHODS

Cells and viruses. Primary ovine cells (OFTu, for ovine fetal turbinate) were maintained in minimal essential medium (MEM) supplemented with 10% fetal bovine serum (FBS), 2 mM L-glutamine and containing gentamicin (50 μg/ml), penicillin (100 IU/ml), and streptomycin (100 μg/ml). HeLa cells stably expressing green fluorescent protein (GFP) (GFP/HeLa) or ORFV121-GFP (121GFP/HeLa) fusion protein were established as previously described (11) and maintained in Dulbecco's modified essential medium (DMEM) supplemented with 10% FBS, 2 mM L-glutamine, gentamicin (50 μg/ml), penicillin (100 μg/ml), streptomycin (100 μg/ml), and neomycin (G418; 500 μg/ml; Gibco). ORFV strain OV-IA82 (10) was used to construct an *ORFV121* deletion mutant virus (OV-IA82Δ121) in all procedures involving wild-type virus infection and in the cloning of viral genes. OV-IA82Δ121 was used to construct an *ORFV121* revertant virus (OV-IA82Rv121).

Plasmids. *ORFV121* coding sequence was PCR amplified from the OV-IA82 genome with primers 121Flag-Fw(HindIII) (5′-TAAGGCCTCTAAGCTTATGGCTGGCTTCCTAGGCGCGTTC-3′), 121Flag-Rv(XhoI) (5′-CAGAATTCGCCTCGAGCAGAACTTCCTCCACTTTGCAGCA-3′), 121EGFP-Fw(XhoI) (5′-ACTTACACTCGAGCAACCATGGCTGGCTTC-3′), and 121EGFP-Rv(HindIII) (5′-CGTCGCAAGCTTCAGAACTTCCTCCACTTTG-3′) and was cloned into plasmids pCMVTag4A (Stratagene, La Jolla, CA) and pEGFP-N1 (Clontech, Mountain View, CA) to obtain the expression vectors pCMV121Flag and p121EGFP, respectively.

ORFV121 left (LF; 1,016 bp) and right (RF; 853 bp) flanking regions were PCR amplified from the OV-IA82 genome and cloned into the plasmid pZippy-Neo/Gus (14) to obtain the recombination vector pZippy-121LF-Neo/Gus-121RF. PCR primers were 121LF-Fw(SpeI) (5′-TAAGGCCTCTACTAGTCTGCGACCGACATCGCACACATGA-3′), 121LF-Rv(HindIII) (5′-CAGAATTCGCAAGCTTGGTTGTGTGGGCCACAGAGTTGAG-3′), 121RF-Fw(NotI) (5′-ATTCTTATGCGGCCGCGCAGCACTGCTCGGAGGAGTGCTC-3′), and 121RF-Rv(BglII) (5′-CAGAATTCGCAGATCTATCATGCGCAGCGACGACATCATC-3′).

ORFV121 and its left and right flanking regions were PCR amplified from the OV-IA82 genome and cloned into the recombination vector pZippy (14) lacking the Neo/Gus reporter genes. The resultant recombination plasmid pZippy-LF/ORFV121/RF was used to generate the revertant OV-IA82Rv121 virus. PCR primers used for amplification were described above [121LF-Fw(HindIII) and 121RF-Rv(BglII)]. The DNA sequencing of plasmid constructs confirmed the integrity of OV-IA82 sequences in the recombination plasmids and in-frame cloning of ORFV121 with Flag and GFP fusion proteins.

RT-PCR. The transcription kinetics of *ORFV121* were examined during ORFV replication in OFTu cells by reverse transcription-PCR (RT-PCR). Cells were inoculated with OV-IA82 (multiplicity of infection [MOI], 10) in the presence or absence of cytosine arabinoside (AraC; 40 μg/ml) and harvested at 0, 1, 2, 3, 6, 12, and 24 h postinoculation (p.i.). RNA samples were processed and reverse transcribed as previously described (11). The transcription of *ORFV121*, *ORFV024* (early control gene), and *ORFV059* (late control gene) was assessed by PCR using primers 121Fw (5′-TCCAGCTGCCCGCGACGACGCGC-3′), 121Rv (5′-GGAGGTTGGGTCTGCCGGCGCCGCA-3′), 024Fw (5′-GCGGACACAGCCACAACCACAGTC-3′), 024Rv (5′-CTAGCACGCGCTTTCGGTACCGCC-3′), 059Fw (5′-ATGGATCCACCCGAAATCAC-3′), and 059Rv (5′-TCACACGATGGCCGTGACCAGC-3′), respectively.

Confocal microscopy. OFTu cells cultured on glass coverslips were transiently transfected with plasmid pEGFP-N1 or p121EGFP and subsequently infected with OV-IA82Δ121 (24 h posttransfection). Cells were fixed, stained with 4′,6′-diamidino-2-phenylindole (DAPI), and examined by confocal microscopy at 6 h p.i. To investigate a potential colocalization of ORFV121 and NF-κB-p65, OFTu cells were transiently transfected with (i) pEGFP-N1 (control vector) and pT7NF-κB-p65 or (ii) p121EGFP and pT7NF-κB-p65, and then they were treated with TNF-α for 60 min. After fixation and permeabilization, cells were probed with an anti-NF-κB-p65 antibody (no. 3034; Cell Signaling, Danvers, MA), incubated with a secondary goat anti-rabbit antibody (Alexa Fluor 594; no. A31631; Invitrogen), and examined by confocal microscopy.

Construction and characterization of *ORFV121* deletion mutant virus OV-IA82Δ121 and *ORFV121* revertant virus OV-IA82Rv121. *ORFV121* deletion mutant OV-IA82Δ121 virus was generated by homologous recombination between OV-IA82 and the recombination vector pZippy-121LF-Neo/Gus-121RF (11). The absence of *ORFV121* sequence and the presence of Neo/Gus sequences in the purified recombinant virus were determined by PCR and Southern blotting.

ORFV121 revertant virus OV-IA82Rv121 was generated by homologous re-

combination between the deletion mutant virus OV-IA82Δ121 and the recombination vector pZippy-LF/ORFV121/RF. The construction, selection, and purification of OV-IA82Rv121 were performed as previously described (12). The presence of *ORFV121* sequence and the absence of Neo/Gus sequences in the purified revertant virus were determined by PCR and Southern blotting. The integrity and identity of the OV-IA82 sequences flanking the recombination regions were confirmed by DNA sequencing.

Real-time PCR analysis. The gene expression of OFTu cells in response to ORFV infection was examined by real-time PCR. OFTu cells cultured in 35-mm dishes for 16 h were mock infected or infected with OV-IA82 or OV-IA82Δ121 (MOI, 10). Cells were harvested at 2 and 4 h p.i. and subjected to RNA extraction and reverse transcription as previously described (11). The expression of genes for *interleukin-1*α (*IL-1*α), *IL-6*, *IL-8*, *NF-κBIA*, *CCL20*, *CXCL3*, *IRF-1*, *ICAM-1*, and *PTGS2* was assessed using primers and probes synthesized based on ovine gene sequences in GenBank (TaqMan gene expression custom assays; Applied Biosystems). Real-time PCR conditions and data analysis were performed as previously described (11).

NF-κB luciferase assays. The effect of ORFV121 on NF-κB-mediated transcription was investigated during ORFV infection in cell cultures. OFTu cells cultured in 12-well plates (1.2×10^5 cells per well) were cotransfected with the vectors pNF-κB-Luc (450 ng; Clontech, Montain View, CA) and pRL-TK (50 ng; Promega, Madison, WI) using Lipofectamine 2000 (Invitrogen). Cells were mock infected (MEM) or infected with OV-IA82, OV-IA82Δ121, or OV-IA82Rv121 (MOI, 10) at 24 h posttransfection. Luciferase activities were determined at 2, 4, and 6 h p.i. using the dual luciferase reporter assay (Promega) and a luminometer.

The ability of ORFV121 to inhibit NF-κB-transcriptional activity induced by LPS and TNF-α was investigated. OFTu cells were cotransfected with pNF-κB-Luc (450 ng; Clontech), pRL-TK (50 ng; Promega), and pCMV121Flag (500 ng) or control empty vector pCMVTag4A (500 ng) using Lipofectamine 2000 (Invitrogen). Cells were exposed to control medium (MEM, 2% FBS) or medium containing LPS (250 ng/ml; Invivogen, San Diego, CA) for 6 h at 24 h posttransfection. Luciferase activities were determined as described above.

Stable cell lines expressing GFP (GFP/HeLa) or ORFV121-GFP (121GFP/HeLa) were cotransfected with pNF-κB-Luc (450 ng; Clontech) or pRL-TK (50 ng; Promega) and exposed to control medium (DMEM, 2% FBS) or medium containing TNF-α (20 or 50 ng/ml; Cell Signaling, Danvers, MA) for 6 h. Cells were harvested and luciferase activities determined as described above. Firefly luciferase activity was normalized to the sea pansy luciferase activity, and resultant ratios were used to calculate fold changes in luciferase activity. All transfections were performed in triplicate, and the means of the three replicates were used to calculate fold changes. The statistical analysis of the data was performed by using Student's *t* test.

Western immunoblotting. The effect of ORFV121 on the NF-κB signaling pathway was investigated by Western immunoblotting. Cells stably expressing GFP (GFP/HeLa) or ORFV121-GFP (121GFP/HeLa) were cultured in six-well plates for 48 h, exposed to control medium (DMEM, 2% FBS) or medium containing TNF-α (20 ng/ml) for 5 and 15 min, and lysed as described above. OFTu cells cultured in six-well plates were transfected with pCMV121Flag (2 μg) or with control empty vector pCMVTag4A (2 μg) using Lipofectamine 2000. Cells were exposed to control medium (MEM, 2% FBS) or medium containing TNF-α (20 ng/ml) for 5 and 15 min and lysed as described above at 24 h posttransfection. OFTu cells cultured in six-well plates were inoculated with OV-IA82, OV-IA82Δ121, or OV-IA82Rv121 (MOI, 10) and harvested at various times p.i. (15, 30, and 60 min). Uninfected cells were used as controls.

In the experiments described above, 50 μg of protein extract was resolved by SDS-PAGE (11). Antibodies used include IκBα (sc-371; Santa Cruz), phospho-IκBα (Ser32/36) (no. 9246; Cell Signaling), NF-κB-p65 (no. 3034; Cell Signaling), phospho-NF-κB-p65 (Ser536) (no. 3033; Cell Signaling), glyceraldehyde-3-phosphate dehydrogenase (GAPDH) (sc-25778; Santa Cruz), Flag-M2 (no. 200471; Stratagene), or GFP (sc-8334; Santa Cruz). The densitometric analysis of the blots was performed by using ImageJ software, version 1.62 (National Institutes of Health, Bethesda, MD). The statistical analysis of the data was performed by using Student's *t* test.

Cytoplasmic and nuclear cell fractionation. GFP/HeLa and 121GFP/HeLa stable cell lines cultured in six-well plates for 48 h were treated with TNF-α (20 ng/ml) for 1 h and harvested in phosphate-buffered saline (PBS). Untreated cells were used as controls. OFTu cells cultured in six-well plates were mock infected or infected with OV-IA82, OV-IA82Δ121, or OV-IA82Rv121 and harvested at 60 min p.i. Cytoplasmic and nuclear protein fractions were extracted with a ProteoJet cytoplasmic and nuclear protein extraction kit (Fermentas, Glen Burnie, MD) by following the manufacturer's protocol. Approximately 20 μg of cytoplasmic and nuclear protein extract was resolved by SDS-PAGE and blotted to nitrocellulose membranes, and blots were probed with antibodies against NF-κB-p65 (no. 3034; Cell Signaling), GAPDH (sc-25778; Santa Cruz), or histone H3 (sc-10809; Santa Cruz).

Immunoprecipitation. The interaction of ORFV121 with NF-κB-p65 was assessed by using coimmunoprecipitation assays. OFTu cells were cotransfected with either (i) pCMVTag4A and pT7NF-κB-p65 or (ii) pCMV121Flag and pT7NF-κB-p65, and they were exposed to control medium or medium containing TNF-α (20 ng/ml) for 15 min at 24 h posttransfection. Cells were lysed with 200 μl of lysis buffer (50 mM Tris-HCl, pH 7.4, with 150 mM NaCl, 1 mM EDTA, and 1% Triton X-100) and incubated at room temperature for 15 min. Proteins were immunoprecipitated by using the FLAG immunoprecipitation kit (Sigma, St. Louis, MO) by following the manufacturer's protocol or an anti-NF-κB-p65 antibody coupled to protein G agarose beads (Upstate) as previously described (12). Immunoprecipitated proteins were resolved by SDS-PAGE, and blots were probed with antibodies against Flag-M2 (no. 200471; Stratagene) and NF-κB-p65 (no. 3034; Cell Signaling) as described above.

Animal inoculations. The effect of *ORFV121* on ORFV virulence and pathogenesis was investigated in lambs. Three- to 5-month-old crossbreed lambs acquired from an orf-free flock were allocated in five groups distributed in two independent experiments. Experiment 1 (exp 1) consisted of mock-infected (n = 2), OV-IA82-infected (n = 2), and OV-IA82Δ121-infected lambs (n = 2), and experiment 2 (exp 2) consisted of OV-IA82-infected (n = 3), OV-IA82Δ121-infected (n = 3), and OV-IA82Rv121-infected lambs (n = 3). Animals were tranquilized with xilazine (Rompun; Bayer), and sites of inoculation were cleaned with water. After the scarification of the mucocutaneous junction of the inferior lips and the skin of the axillary (exp 1) or the inner (exp 2) side of the thighs, 0.25 ml of virus suspension containing $10^{7.3}$ 50% tissue culture infectious doses/ml was inoculated at each site by using a cotton swab. Animals were monitored for 19 days for characteristic orf lesions, including erythema, vesicles, pustules, and scabs. Skin biopsy specimens were collected from the thighs (exp 2) at days 1, 2, 3, 5, and 19 p.i, fixed in 10% buffered formalin, embedded in paraffin, sectioned (4 μm), and stained with hematoxylin and eosin using standard methods. Histological sections were examined for the presence of epidermal hyperplasia, ballooning degeneration of keratinocytes, hyper- and parakeratosis, intraepidermal microabcesses, rete ridge formation, keratinocyte intracytoplasmic inclusion bodies, and the infiltration of epidermis and underlying dermis with neutrophils and mononuclear cells. All animal procedures have been revised and approved by the University of Nebraska–Lincoln Institutional Animal Care and Use Committee (protocol no. 214 as of 23 January 2008).

RESULTS

ORFV *ORFV121* is transcribed early-late during ORFV infection, and the protein localizes to the cell cytoplasm. ORFV *ORFV121* encodes a protein of 300 to 306 amino acids in length with a predicted molecular mass of 34 kDa. ORFV strain IA82 ORFV121 (AAR98216.1) is highly conserved among ORFV isolates, sharing 98, 96, and 88% amino acid identity with its homologues in the sheep ORFV isolates Orf11 (AAO91831.1) and NZ2 (ABA00639.1) and the goat ORFV isolate SA00 (NP_957898.1), respectively. Notably, the pseudocowpoxvirus (PCPV) reference strain VR634 ORF121 homologue (ADC54021; 70% amino acid identity) lacks most of the amino-terminal region of the protein (ORFV IA82 ORF121 positions 4 to 145), while the reindeer PCPV isolate F00.120R lacks an *ORF121* gene (22). The most divergent parapoxvirus (PPV) ORF121 homolog, BPSV strain AR02 BPSV121 (NP_958029.1; 39% amino acid identity), contains three unique insertions in the amino-terminal region of the protein (ORFV IA82 ORF121 positions 24 to 27, 42 to 46, and 87 to 92), a 27-amino acid deletion in the middle of the protein (positions 132 to 158), and two additional deletions in the carboxyl terminal of the protein (positions 204 to 208 and 285 to 300). A 60-amino-acid region at the carboxyl termini of PPV ORF121 proteins exhibits the highest sequence conservation (ORFV IA82 ORF121 position 218 to 278; ≥75%). PPV ORF121 lacks homology to other known proteins of viral or

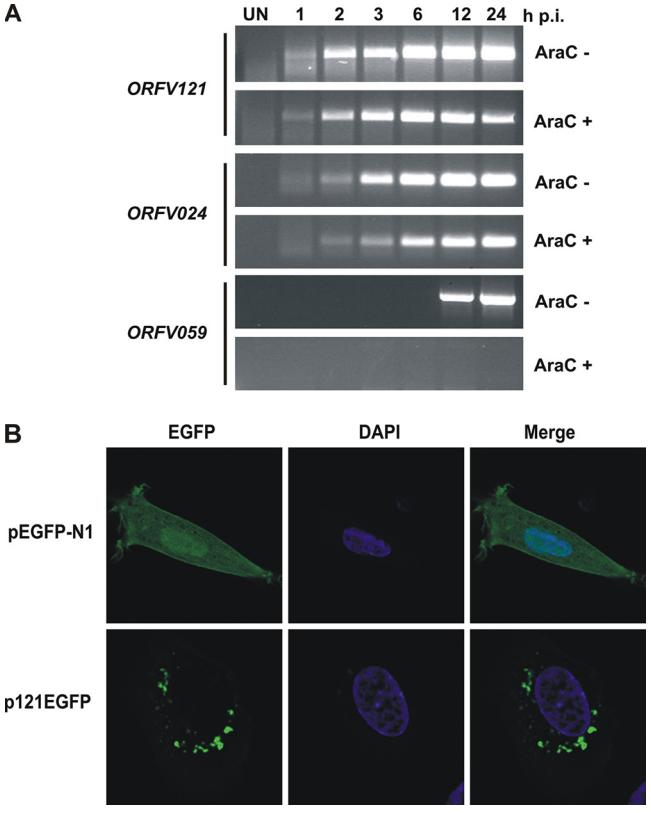

FIG. 1. Transcription kinetics and subcellular localization of ORFV121. (A) Transcription kinetics of *ORFV121*, *ORFV024* (early gene control), and *ORFV059* (late gene control) during ORFV infection in OFTu cells in the presence (+) or absence (−) of AraC as determined by RT-PCR. (B) Subcellular localization of ORFV121 in OFTu cells transfected with plasmids encoding GFP (pEGFP-N1) or ORFV121-GFP (pEGFP121) and subsequently infected with OV-IA82Δ121 (MOI, 10). Cells were stained with DAPI and examined by confocal microscopy (6 h p.i.).

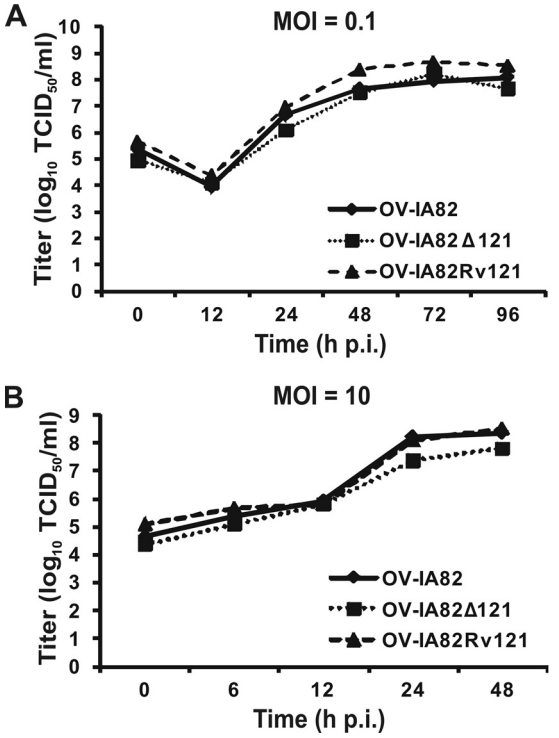

FIG. 2. Replication characteristics of *ORFV121* deletion mutant virus OV-IA82Δ121. Shown are multiple-step (A) and one-step (B) growth curves of wild-type (OV-IA82), deletion mutant (OV-IA82Δ121), and revertant (OV-IA82Rv121) virus in primary OFTu cells (MOI, 0.1 and 10, respectively).

cellular origin, and no motifs or domains suggestive of putative protein function were identified.

ORFV121 transcription kinetics was investigated during ORFV replication in OFTu cells by RT-PCR. *ORFV121* transcription was detected throughout the ORFV infection cycle (1 to 24 h p.i.) and was decreased at 12 and 24 h p.i. in the presence of AraC, an inhibitor of DNA replication and of late poxviral gene transcription (Fig. 1A). These results indicate that *ORFV121* is an early-late poxviral gene.

The subcellular localization of ORFV121 was investigated in OFTu cells transiently expressing ORFV121-GFP and subsequently infected with the *ORFV121* deletion mutant virus OV-IA82Δ121. ORFV121-GFP localized to the cell cytoplasm, exhibiting a punctate distribution pattern (Fig. 1B). No colocalization of ORFV121 with markers for endoplasmic reticulum and mitochondria was observed (data not shown).

***ORFV121* is nonessential for ORFV replication *in vitro*.** Replication properties of OV-IA82, OV-IA82Δ121, and OV-IA82Rv121 were examined *in vitro*. No differences in replication kinetics and viral yields were observed when multiple-step or one-step growth curves of OV-IA82Δ121 were compared to those of the revertant OV-IA82Rv121 or wild-type OV-IA82 virus in OFTu (Fig. 2A and B) or in HeLa cell cultures (data not shown). Additionally, no differences in cytopathic effect and plaque size and morphology were observed for OV-IA82, OV-IA82Δ121, and OV-IA82Rv121 in OFTu cells (data not shown). Thus, *ORFV121* is nonessential for ORFV replication in OFTu and in HeLa cell cultures.

OV-IA82Δ121 infection results in increased expression of NF-κB-regulated genes in primary OFTu cells. The preliminary microarray screening of OV-IA82Δ121-infected OFTu cells indicated the increased expression of genes regulated by the NF-κB family of transcription factors (data not shown). The real-time PCR analysis of OV-IA82Δ121-infected OFTu cells at 2 h p.i. confirmed a marked increase in the expression of NF-κB-regulated genes *IL-1*-α (24.4-fold), *IL-6* (14.7-fold), *IL-8* (28.2-fold), *NFκBIA* (6.8-fold), *CCL20* (51.1-fold), *CXCL3* (49.1-fold), *IRF-1* (4.3-fold), *ICAM-1* (4.5-fold), and *PTGS2* (8.4-fold) compared to that of mock-infected or wild-type virus-infected cells (Fig. 3A). The expression of these genes was similarly increased in OV-IA82Δ121-infected cells at 4 h p.i. (data not shown). No significant differences in expression levels were observed between mock- and wild-type virus-infected cells (Fig. 3A).

The ability of ORFV121 to inhibit NF-κB-mediated transcription was further investigated by using an NF-κB-luciferase reporter assay. Infection with OV-IA82Δ121 virus resulted in a marked and significant increase in luciferase activity of up to 4.8 ($P < 0.01$), 11.0 ($P < 0.005$), and 7.6-fold ($P < 0.005$) at 2, 4, and 6 h p.i., respectively (Fig. 3B). The restoration of

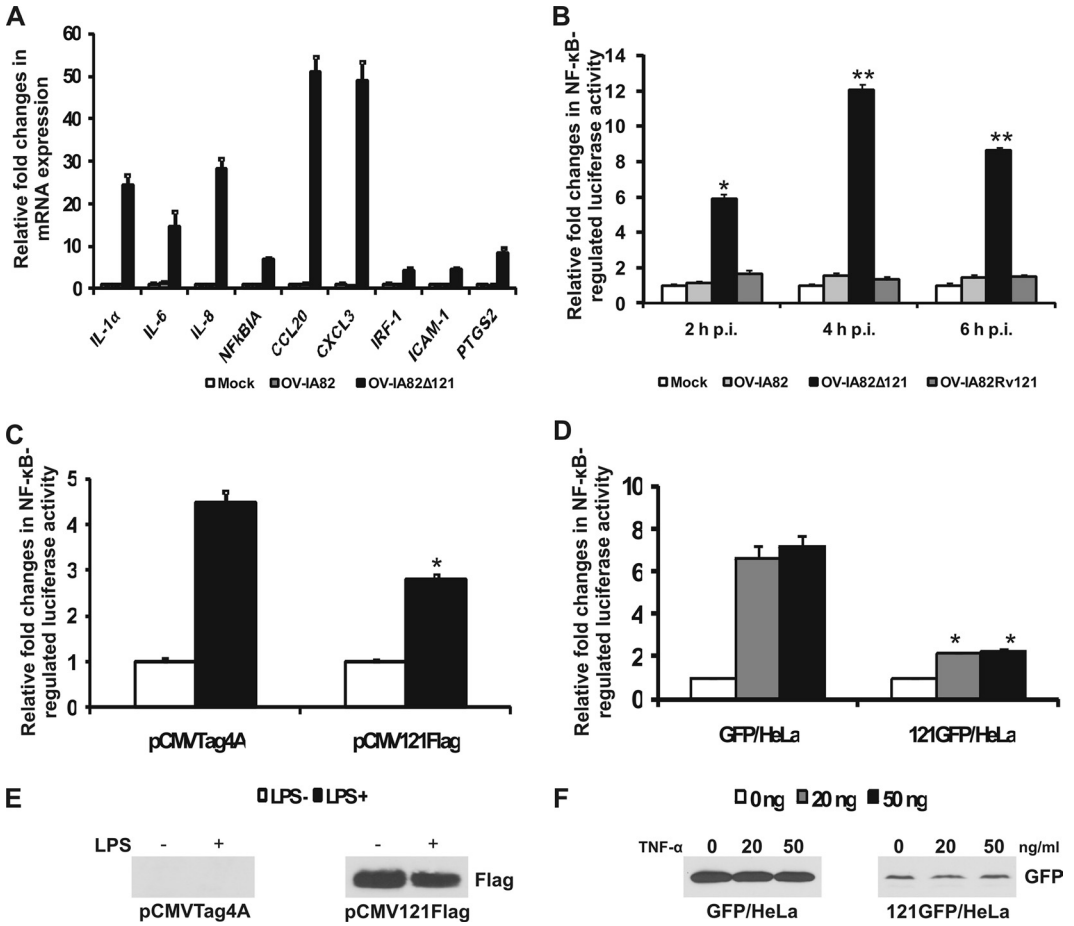

FIG. 3. Effect of ORFV121 on NF-κB-regulated gene transcription. (A) OFTu cells were infected with OV-IA82 or OV-IA82Δ121 (MOI, 10) or were mock infected, and the expression of selected NF-κB-regulated genes was determined by real-time PCR at 2 h p.i. (B) OFTu cells were cotransfected with plasmids pNF-κB*Luc* and pRL-TK and subsequently infected with OV-IA82, OV-IA82Δ121, or OV-IA82Rv121 (MOI, 10) or were mock infected. Firefly and sea pansy luciferase activities were measured at 2, 4, and 6 h p.i. and expressed as relative fold changes in luciferase activity (*, $P < 0.01$; **, $P < 0.005$). (C) OFTu cells were cotransfected with plasmids pNF-κB*Luc*, pRL-TK, and either pCMVTag4A or pCMV121Flag and subsequently were treated with LPS (250 ng/ml) for 6 h. Luciferase activities were determined as described for panel B (*, $P = 0.01$). (D) HeLa cells stably expressing GFP (GFP/HeLa) or ORFV121-GFP (121GFP/HeLa) were cotransfected with plasmids pNF-κB*Luc* and pRL-TK and subsequently treated with TNF-α (20 or 50 ng/ml) for 6 h. Luciferase activities were determined as described for panel B (*, $P < 0.05$). (E) Expression of ORFV121-Flag in samples examined in panel C, as determined by Western blotting. (F) Expression of GFP and ORFV121-GFP in samples examined in panel D, as determined by Western blotting. The results are representative of two (C) or three (A, B, and D) independent experiments.

ORFV121 in the revertant virus (OV-IA82Rv121) rescued the wild-type virus phenotype (Fig. 3B). Taken together, these data indicate that ORFV121 inhibits NF-κB-mediated transcription during ORFV infection in OFTu cells.

Expression of ORFV121 decreases NF-κB-mediated transcription induced by LPS and TNF-α. OFTu cells transiently expressing or HeLa cells stably expressing ORFV121 were stimulated with LPS and TNF-α, respectively, and assayed for NF-κB-mediated luciferase activity. The transient expression of ORFV121-Flag in OFTu cells significantly decreased LPS-induced NF-κB-luciferase activity by ~1.7-fold ($P = 0.01$) compared to that of control cells transfected with the empty vector (Fig. 3C and E). Additionally, the stable expression of ORFV121-GFP in HeLa cells markedly decreased TNF-α-induced NF-κB-mediated luciferase activity by ~3.5-fold ($P < 0.05$) compared to that of control GFP-expressing cells (Fig. 3D and F). These results indicate that ORFV121 inhibits NF-κB-mediated transcription following the stimulation of cells with LPS and TNF-α, two potent NF-κB inducers.

ORFV121 decreases phosphorylation and nuclear translocation of NF-κB-p65 but does not affect upstream phosphorylation of IκBα. The effect of ORFV121 on the phosphorylation and nuclear translocation of NF-κB-p65 and on the phosphorylation of IκBα was investigated. HeLa cells stably expressing ORFV121-GFP, OFTu cells transiently expressing ORFV121-Flag, and control cells were treated with TNF-α and harvested at various times posttreatment. ORFV121 expression markedly decreased the TNF-α-induced phosphorylation of NF-κB-p65 in both ORFV121 stably and transiently expressing cells (Fig. 4A to D). To assess whether the decreased levels of phospho-NF-κB-p65 detected in ORFV121-expressing cells were due to its effects on events upstream of NF-κB-p65, the phosphorylation levels of IκBα were investigated. ORFV121

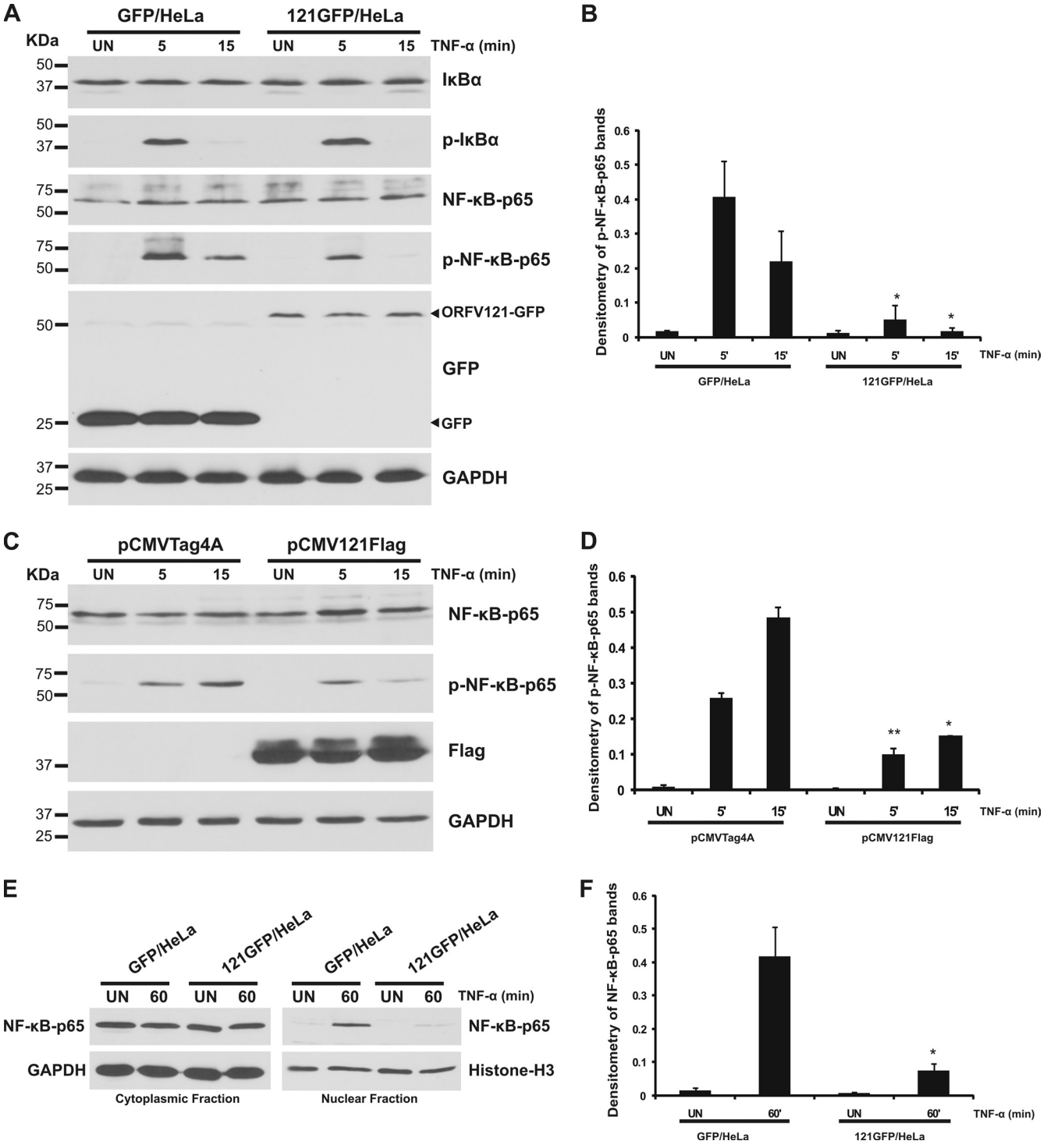

FIG. 4. Effect of ORFV121 on activation of the NF-κB signaling pathway and on nuclear translocation of NF-κB-p65. (A) HeLa cells stably expressing GFP (GFP/HeLa) or ORFV121-GFP (121GFP/HeLa) were treated with TNF-α (20 ng/ml) and harvested at the indicated times (UN, untreated controls). Protein extracts (50 μg) were resolved by SDS-PAGE, blotted, and probed with antibodies directed against proteins indicated on the right. (B) Densitometry of phospho-NF-κB-p65 bands normalized to the levels for the control GAPDH (*, $P < 0.05$). (C) OFTu cells transiently transfected with plasmid pCMVTag4A or pCMV121Flag were treated with TNF-α (20 ng/ml) and harvested at the indicated times (UN, untreated controls). Protein extracts (50 μg) were resolved by SDS-PAGE, blotted, and probed with antibodies directed against proteins indicated on the right. (D) Densitometry of phospho-NF-κB-p65 bands normalized to the levels for the control histone H3 (*, $P < 0.05$; **, $P < 0.005$). (E) HeLa cells stably expressing GFP (GFP/HeLa) or ORF121-GFP (121GFP/HeLa) were treated with TNF-α (20 ng/ml) for 60 min, and cytoplasmic and nuclear protein fractions were extracted (UN, untreated controls). Protein extracts (20 μg) were resolved by SDS-PAGE, blotted, and probed with antibodies against NF-κB-p65 (top), GAPDH (bottom left), or histone H3 (bottom right). (F) Densitometry of NF-κB-p65 bands normalized to loading control histone H3 (*, $P < 0.05$). The results (A to F) are representative of three independent experiments.

expression did not affect the TNF-α-induced phosphorylation of IκBα (Fig. 4A).

The effect of ORFV121 expression on the translocation of NF-κB-p65 to the nucleus was investigated by using Western immunoblotting and confocal microscopy. HeLa cells stably expressing ORFV121-GFP and control cells expressing GFP alone were stimulated with TNF-α for 60 min, and cytoplasmic and nuclear cell fractions were obtained. ORFV121 expression markedly decreased the nuclear translocation of NF-κB-p65 compared to that of control cells (Fig. 4E and F). Reduced levels of phospho- or nuclear-translocated NF-κB-p65 in ORFV121-expressing cells were not due to protein degradation, since levels of pan-NF-κB-p65 and glyceraldehyde-3-phosphate dehydrogenase (GAPDH) (Fig. 4A and C) or histone H3 (Fig. 4E) were constant in all samples. The levels of nuclear-translocated NF-κB-p65 in GFP/HeLa cells were not due to leakage from the cytoplasmic fraction, since NF-κB-p65 was not detected in the nuclear fraction of control untreated cells (Fig. 4E). Similarly, the transient expression of ORFV121 in TNF-α-treated OFTu cells markedly reduced the nuclear translocation of NF-κB-p65 (see Fig. 6A). Taken together, these results indicate that ORFV121 functions downstream of IκBα by inhibiting the phosphorylation and nuclear translocation of NF-κB-p65.

ORFV121 decreases phosphorylation and nuclear translocation of NF-κB-p65 during ORFV infection in OFTu cells. The ability of ORFV121 to suppress the phosphorylation and nuclear translocation of NF-κB-p65 during ORFV infection in OFTu cells was investigated. OFTu cells were mock infected or infected with OV-IA82, OV-IA82Δ121, or OV-IA82Rv121 and harvested at various times p.i. Infection with the wild-type virus OV-IA82 resulted in low levels of NF-κB-p65 phosphorylation (Fig. 5A and B). OV-IA82Δ121 infection induced a marked increase in NF-κB-p65 phosphorylation as detected at 60 min p.i. (Fig. 5A and B). The restoration of *ORFV121* in the revertant virus (OV-IA82Rv121) rescued the wild-type virus phenotype (Fig. 5A and B). To assess the nuclear translocation of NF-κB-p65 during ORFV infection, OFTu cells were mock infected or infected with OV-IA82, OV-IA82Δ121, or OV-IA82Rv121 and fractionated, and cytoplasmic and nuclear cell extracts were analyzed by Western immunoblotting. Infection with wild-type and revertant viruses resulted in similar low levels of NF-κB-p65 in the nucleus, whereas OV-IA82Δ121 infection markedly increased the nuclear translocation of NF-κB-p65 (Fig. 5C and D). Taken together, these results indicate that *ORFV121* suppresses the phosphorylation and nuclear translocation of NF-κB-p65 during ORFV infection.

ORFV121 interacts with NF-κB-p65. The interaction of ORFV121 and NF-κB-p65 was investigated as a potential mechanism for ORFV121 inhibitory effect on the NF-κB signaling pathway. OFTu cells were cotransfected with expression vectors p121EGFP and pT7-NFκBp65 and treated with TNF-α for 60 min, and the localization of these proteins was assessed by confocal microscopy. ORFV121 colocalized with NF-κB-p65 in the cytoplasm of transfected cells, suggesting an interaction between ORFV121 and NF-κB-p65 (Fig. 6A). The specific interaction of ORFV121 and NF-κB-p65 was further investigated by using coimmunoprecipitation assays. OFTu cells cotransfected with pT7-NFκBp65 and either pCMVTag4A or pCMV121Flag were treated with TNF-α and harvested at 15 min posttreatment. Reciprocal immunoprecipitation assays with either anti-Flag (Fig. 6B) or anti-NF-κB-p65 (Fig. 6C) antibody resulted in the coprecipitation of ORFV121-Flag and NF-κB-p65. A potential interaction of ORFV121-Flag with NF-κB-p50 also was investigated by using coimmunoprecipitation assays. No association of ORFV121-Flag with NF-κB-p50 was detected (data not shown). These results indicate that ORFV121 physically interacts with NF-κB-p65.

ORFV121 contributes to ORFV virulence in sheep. To investigate the effect of ORFV121 on ORFV virulence and pathogenesis, 3- to 5-month-old lambs were inoculated with OV-IA82, OV-IA82Δ121, OV-IA82Rv121, or MEM (control group; exp 1) and monitored for clinical orf. Characteristic orf lesions were observed in all wild-type and revertant virus-inoculated lambs. Lesions were observed initially by day 3 p.i. and consisted of erythema, pustules (day 5 p.i.), and scabs at later times p.i. (6 to 7 days p.i) (Fig. 7). Local scabby tissue deposition was first observed by day 5 p.i. and continued until day 10 p.i. Lesions began to resolve by day 15 p.i., and by day 19 p.i. only the lesion margins were partially covered with scabs. In contrast, lesions induced by the OV-IA82Δ121 virus were less severe and resolved sooner than those induced by wild-type and revertant viruses (exp 1, two of two; exp 2, three of three). Lesions were characterized by erythema, small vesicles, and limited scab formation (Fig. 8A). Erythema was observed initially at day 3 p.i., evolving into pustules (5 days p.i.) that persisted until day 8 p.i. Scabby tissue formation was markedly reduced, with no scabs observed beyond day 10 p.i. A similar low-severity and short-duration disease was observed in lambs inoculated with OV-IA82Δ121 in the axillary region (exp 1) or in the inner side of the thighs (exp 2) (data not shown). Control group animals did not exhibit significant changes, and minor scabs induced by skin scarification were resolved by day 4 p.i. (data not shown). These results indicate that *ORFV121* contributes to ORFV virulence and pathogenesis in the natural host.

Deletion of *ORFV121* from the ORFV genome results in a reduced cellular inflammatory response in the skin. To compare histological changes induced by OV-IA82, OV-IA82Δ121, and OV-IA82Rv121 viruses, lambs were inoculated in the inner side of the thighs, and skin biopsy specimens were collected at 1, 2, 3, 5, and 19 days p.i. No changes other than the partial loss of epidermis and neutrophil infiltration associated with scarification were observed in mock-infected control lambs on days 1 and 2 p.i. (data not shown). Typical histological changes associated with ORFV infection, including epidermal hyperplasia, ballooning degeneration of keratinocytes, skin infiltration with inflammatory cells, pustules, and the accumulation of scabby tissue, were observed in samples from lambs inoculated with OV-IA82 (data not shown), OV-IA82Δ121 (Fig. 8a, b, e, and f), and OV-IA82Rv121 (Fig. 8c, d, g, and h). However, significant differences were observed in the time to appearance and magnitude of changes between OV-IA82Δ121- and OV-IA82Rv121-inoculated groups. By day 3 p.i., all lambs (three out of three) inoculated with OV-IA82Rv121 virus exhibited marked ballooning degeneration of the stratum spinosum of the epidermis (and, occasionally, the external root sheath of hair follicles), infiltration of dermis and epidermis with neutrophils and mononuclear cells, and pustules (Fig. 8c and d). In contrast, ballooning degeneration of keratinocytes and marked

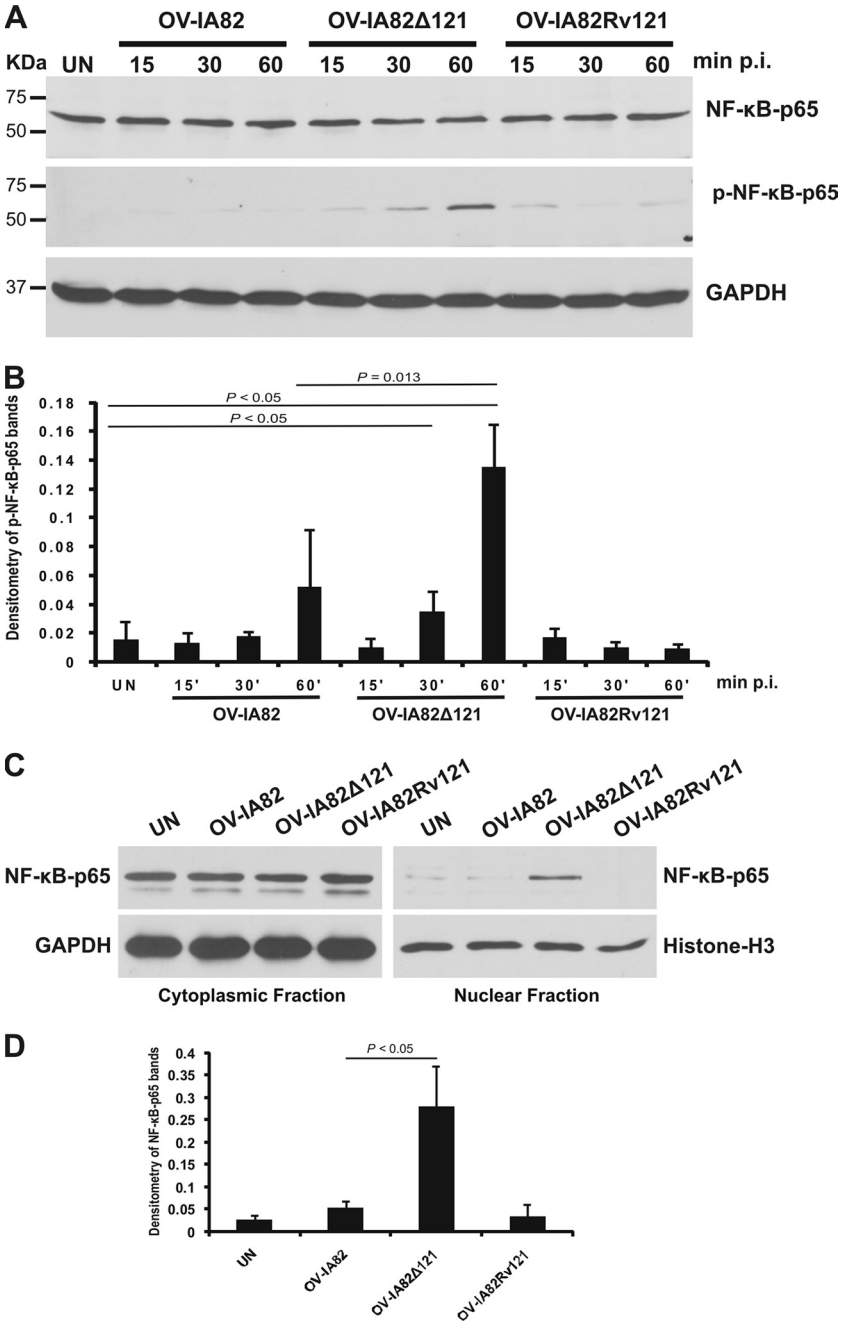

FIG. 5. Effect of ORFV121 on phosphorylation and nuclear translocation of NF-κB-p65 during ORFV infection. (A) OFTu cells were infected with wild-type (OV-IA82), deletion mutant (OV-IA82Δ121), or revertant (OV-IA82Rv121) virus (MOI, 10) and harvested at the indicated times p.i. (UN, uninfected controls). Protein extracts (50 μg) were resolved by SDS-PAGE, blotted, and probed with antibodies directed against proteins indicated on the right. (B) Densitometry of phospho-NF-κB-p65 bands normalized to the levels for the control GAPDH. (C) OFTu cells were infected with wild-type (OV-IA82), deletion mutant (OV-IA82Δ121), and revertant (OV-IA82Rv121) virus (MOI, 10) and harvested at 60 min p.i., and cytoplasmic and nuclear protein fractions were extracted (UN, uninfected controls). Protein extracts (20 μg) were resolved by SDS-PAGE, blotted, and probed with antibodies against NF-κB-p65 (top), GAPDH (bottom left), or histone H3 (bottom right). (D) Densitometry of NF-κB-p65 bands normalized to the levels for the control GAPDH. The results (A to D) are representative of three independent experiments.

skin infiltration with inflammatory cells was observed in only one of three lambs inoculated with OV-IA82Δ121, while pustules were absent (Fig. 8a and b). By day 5 p.i., micropustules were observed in samples from two of three OV-IA82Δ121-infected lambs, while infiltration with inflammatory cells (mostly mononuclear cells) was limited to areas exhibiting ballooning degeneration of keratinocytes (Fig. 8e and f). The accumulation of scabby tissue in OV-IA82Δ121-inoculated lambs was limited or absent. In contrast, lambs infected with OV-IA82Rv121 exhibited massive inflammatory cell infiltration of the dermis and epidermis, pustule formation, epidermal pathology, and accumulation of scabby tissue (Fig. 8g and h).

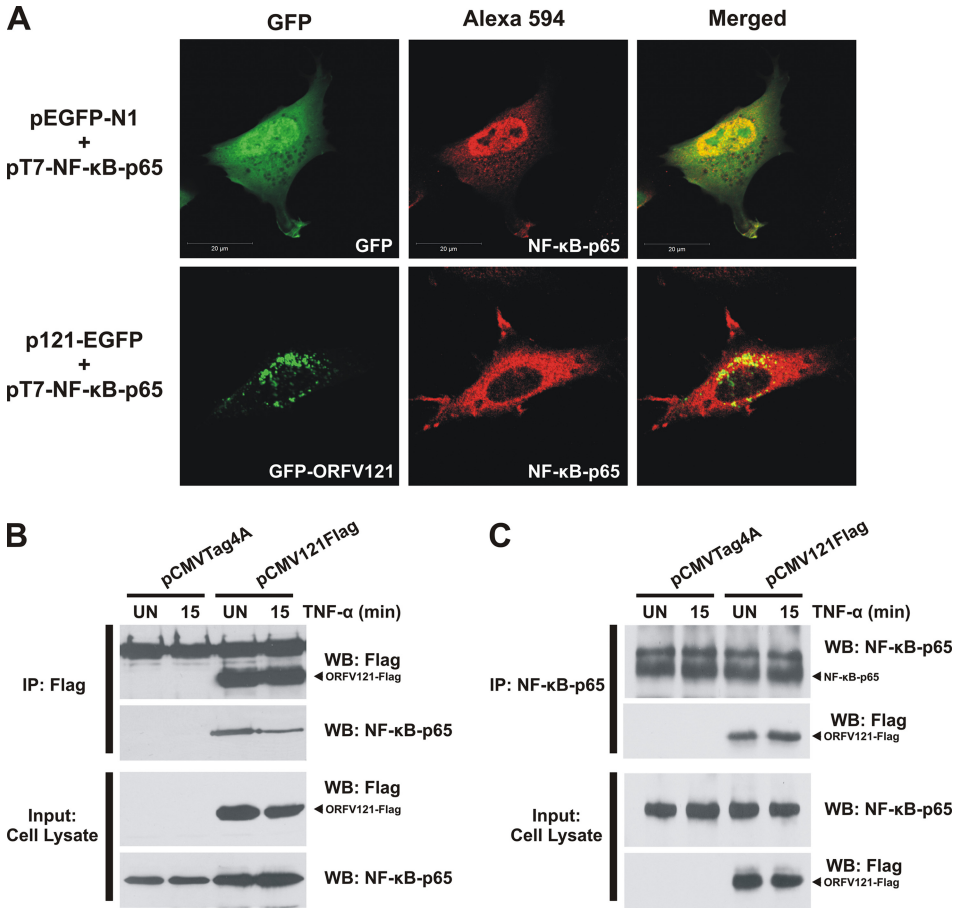

FIG. 6. ORFV121 colocalizes and interacts with NF-κB-p65. (A) OFTu cells were cotransfected with plasmid pNF-κB-p65 and either pEGFP-N1 or p121EGFP. At 24 h posttransfection, cells were treated with TNF-α (20 ng/ml for 60 min), fixed, and examined by confocal microscopy. (B) OFTu cells were cotransfected with plasmid pT7-NF-κB-p65 and either pCMVTagaA (control) or pCMV121Flag (ORFV121-Flag), treated with TNF-α (20 ng/ml), and harvested at 15 min after TNF-α treatment (UN, untreated controls). Protein extracts were immunoprecipitated with anti-Flag antibody coupled to agarose resin and examined by SDS-PAGE-Western blotting (upper) with antibodies directed against proteins indicated on the right. Cell lysates were examined by SDS-PAGE-Western blotting (bottom) with antibodies directed against proteins indicated on the right. (C) OFTu cells were cotransfected with plasmids pT7-NF-κB-p65, pCMVTagaA (control), or pCMV121Flag (ORFV121-Flag), treated with TNF-α (20 ng/ml), and harvested at 15 min after TNF-α treatment (UN, untreated controls). Protein extracts were immunoprecipitated with anti-NF-κB-p65 antibody coupled to protein G agarose beads and examined by SDS-PAGE-Western blotting (upper) with antibodies directed against proteins indicated on the right. Cell lysates were examined by SDS-PAGE-Western blotting (bottom) with antibodies directed against proteins indicated on the right. The immunoprecipitation results shown in B and C are representative of three independent experiments.

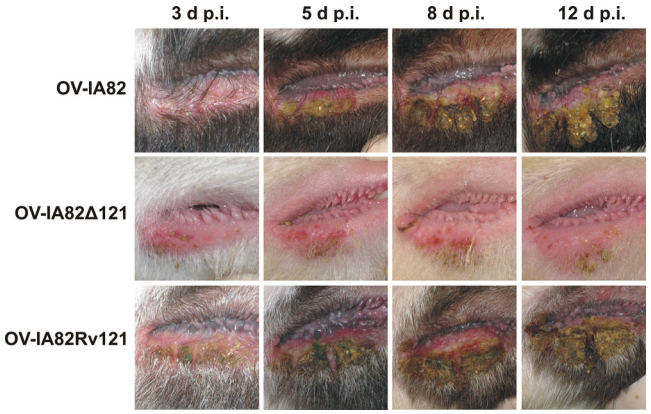

FIG. 7. ORFV121 contributes to virus virulence and pathogenesis in the natural host. (A) Clinical course of orf in lambs inoculated with wild-type (OV-IA82), *ORFV121* deletion mutant (OV-IA82Δ121), or revertant (OV-IA82Rv121) viruses at the mucocutaneus junction of the lower lip (d p.i., days postinfection).

These results indicate that the deletion of ORFV121 from the viral genome results in a reduced epidermal pathology and cellular inflammatory response in the skin.

DISCUSSION

ORFV infection markedly suppresses NF-κB-mediated transcription in primary OFTu cells (11, 12), indicating that this virus efficiently blocks the activation of the NF-κB signaling pathway. Here, the novel ORFV *ORFV121*, a gene unique to parapoxviruses, was shown to encode an inhibitor of NF-κB that contributes to ORFV virulence and disease pathogenesis in sheep. ORFV121 colocalizes and interacts with NF-κB-p65 in the cell cytoplasm, thus providing a mechanism for the inhibition of NF-κB-p65 phosphorylation and nuclear translocation. The deletion of ORFV121 from the ORFV genome resulted in a marked attenuated disease phenotype in sheep,

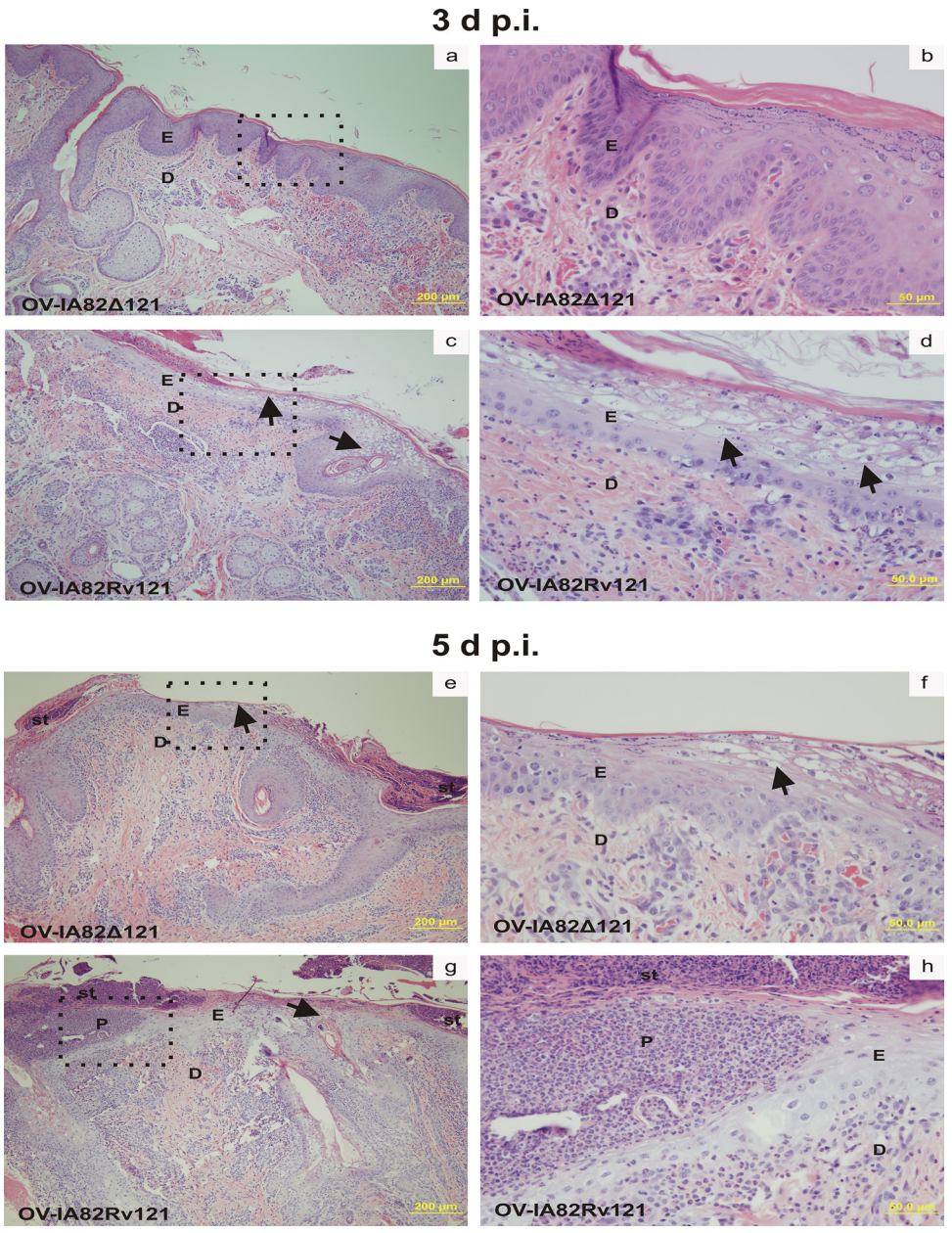

FIG. 8. Histopathological changes in the skin of lambs following infection with OV-IA82Δ121 and OV-IA82Rv121 viruses. Lambs were infected with OV-IA82Δ121 or OV-IA82Rv121 viruses at sites on the inner side of the thighs, and skin biopsy specimens were collected at various days postinoculation and processed for histology. Images are representative of changes at 3 (a to d) and 5 days p.i. (bottom panels e to h). Panels on the right (b, d, f, and h) represent a higher magnification of dotted rectangles highlighting the differences in the histological changes observed between OV-IA82Δ121- and OV-IA82Rv121-inoculated lambs (d, increased ballooning degeneration in keratinocytes and increased inflammatory cell infiltration of the dermis compared to that shown in b; h, increased scabby tissue deposition, pustule formation, and inflammatory cell infiltration compared to that shown in f). E, epidermis; D, dermis; P, pustules; st, scabby tissue; arrows indicate ballooning degeneration. Hematoxylin and eosin staining was used.

indicating that ORFV121 is a *bona fide* virulence determinant for ORFV in the natural host.

ORFV ORFV121, while not affecting the phosphorylation of IκBα, inhibits the phosphorylation (Ser536) and nuclear translocation of NF-κB-p65. Normal levels of phospho-IκBα in ORFV121-expressing cells indicated that the upstream activation of IκB kinases was not affected by ORFV121 and further suggested that ORFV121 functions downstream in the pathway. Consistently with this, ORFV121 colocalized and coprecipitated with NF-κB-p65, indicating that the physical interaction of ORFV121 with NF-κB-p65 is a likely mechanism by which ORFV121 inhibits the phosphorylation, nuclear translocation, and, consequently, transcriptional activity of NF-κB-p65.

Phosphorylation is a critical posttranslational modification that regulates the activity of key components of the NF-κB

signaling pathway, including the transactivating NF-κB subunit NF-κB-p65 (40, 50). Ten phosphorylation sites have been identified in NF-κB-p65, serines 205, 276, 281, 311, 468, 529, and 536 and threonines 254, 435, and 505, many of which have a modulatory role on NF-κB transcriptional activity (40). For example, the phosphorylation of NF-κB-p65 at Ser536 was shown to impair NF-κB-p65-IκBα interaction, which may accelerate the nuclear translocation of NF-κB-p65 (2) or decrease its nuclear export by newly synthesized IκBα, thus regulating the duration of NF-κB-mediated transcription (50). Additionally, the phosphorylation of NF-κB-p65 at serines 276 and 536 is required for the recruitment of the coactivator p300 to the transcriptional complex, thus promoting the full transcriptional activity of NF-κB-p65 (7, 40). The inhibitory effects of ORFV121 on NF-κB-mediated gene transcription observed here likely are due to the decreased phosphorylation and nuclear translocation of NF-κB-p65. However, given the physical interaction between ORFV121 and NF-κB-p65, the possibility that ORFV121 affects additional events regulating the transcriptional activity of NF-κB-p65 cannot be formally excluded.

Most poxviral NF-κB inhibitors identified to date function in the cell cytoplasm mainly by preventing the activation of the IKK complex (reviewed in reference 28), the bottleneck for most NF-κB-activating stimuli (25). However, selected inhibitors encoded by these viruses have been shown to function downstream in the pathway directly on NF-κB subunits (5, 29, 30). For example, myxoma virus (MYXV) M013, variola virus (VARV) G1R and its orthologs in monkeypox virus (MPXV MPXV003), ectromelia virus (ECTV ECTV002), and cowpox virus (CPXV) (CPXV006) were shown to interact with the NF-κB subunit NF-κB-p105, consequently inhibiting the nuclear translocation of NF-κB-p50/NF-κB-p65 (29, 30). Additionally, CPXV-encoded CPXV077 was shown to interact with and inhibit the nuclear translocation of the NF-κB transactivating subunit NF-κB-p65 (5). Here, we have shown that a novel poxviral NF-κB inhibitor encoded by ORFV *ORFV121* targets NF-κB-p65 in the cell cytoplasm. ORFV121 binds to and inhibits the phosphorylation and nuclear translocation of NF-κB-p65. Therefore, targeting NF-κB subunits in the cell cytoplasm and preventing their translocation to the nucleus represents an efficient strategy that selected poxviruses use to inhibit NF-κB transactivating activity.

The NF-κB signaling pathway integrates several aspects of skin homeostasis, including keratinocyte proliferation, differentiation, apoptosis, and innate immune responses (39, 51). This broad spectrum of significant biological activities makes predictions regarding the role of poxviral NF-κB inhibitors in viral host range and pathogenesis difficult. Multiple NF-κB inhibitors encoded by individual poxviruses, including ORFV (e.g., ORFV002, ORFV024, and ORFV121), further complicate this matter. Some poxviral NF-κB inhibitors have been shown to affect virus virulence and disease pathogenesis to some extent; however, the degree of virus attenuation resulting from single-gene deletions has been variable and, in most cases, very modest (1, 8, 10, 11, 21, 48). With a few exceptions (CPXV *CPXV006* and MYXV *M013* and *M150R*), no single-gene deletion rendered marked virus attenuation *in vivo*, suggesting that at the host level multiple NF-κB inhibitors encoded by individual poxviruses exert complementary functions to effectively suppress the NF-κB signaling pathway during virus infection (4, 24, 30, 42).

The deletion of *ORFV121* from the ORFV genome resulted in a marked attenuated disease phenotype in sheep, indicating that ORFV121 is a virulence determinant for ORFV in the natural host. Histological changes and inflammatory responses induced by OV-IA82Δ121 were less severe than those induced by the wild-type or revertant viruses. These results contrast with our findings for ORFV-encoded NF-κB inhibitors ORFV002 and ORFV024, where viruses containing individual gene deletions had no significant effect on ORFV virulence and disease pathogenesis in sheep (11, 12). These observations suggest that, in addition to possible complementary functions, individual NF-κB inhibitors encoded by ORFV modulate distinct cellular processes regulated by the NF-κB signaling pathway during infection *in vivo* (e.g., immune responses, cell proliferation, cell differentiation, and/or apoptosis). While the regulation of some of these processes is essential for virus virulence and disease pathogenesis, the modulation of others may play roles in less understood and perhaps subtle aspects of ORFV host range and infection biology, such as subclinical and/or persistent infections (37).

Results here demonstrating that OV-IA82Δ121 infection induces a reduced inflammatory response in the skin compared to wild-type or revertant virus infection contrast with observations for CPXV- and MYXV-encoded NF-κB inhibitors, CPXV006 and M150R, respectively, for which deletion from the viral genomes resulted in increased inflammatory response at sites of virus replication (4, 30). These findings can be reconciled by the apparently paradoxical roles of the NF-κB signaling pathway in the skin (39). Remarkably, both the continuous activation and/or continuous inhibition of the NF-κB signaling pathway in the epidermis has been shown to result in enhanced skin inflammatory responses (39). Therefore, it is possible that by inhibiting the activation of the NF-κB signaling pathway, ORFV121 stimulates local inflammatory responses following ORFV infection, thus contributing to disease development and pathogenesis. Alternatively, ORFV121 may function in other cellular processes regulated by NF-κB in the skin, such as keratinocyte proliferation, differentiation, and/or apoptosis, potentially contributing to the keratinocyte-restricted host range of ORFV.

Notably, poxviral NF-κB inhibitors that markedly affect virus virulence and disease pathogenesis *in vivo* have been shown to target and/or function directly on NF-κB subunits. For example, CPXV006, a virulence determinant for CPXV in mice, binds to and prevents the degradation of the NF-κB subunit NF-κB-p105 (30). Similarly, MYXV M013, a significant virulence determinant for MYXV in rabbits, has been shown to interact with NF-κB-p105 (24, 42). MYXV M150R, an additional virulence determinant for MYXV in rabbits, was shown to colocalize with NF-κB-p65 in the cell nucleus, although its actual function is unknown (4). ORFV *ORFV121* was shown here to encode a virulence determinant for ORFV in sheep, which binds to and inhibits the phosphorylation and nuclear translocation of NF-κB-p65. These findings suggest that by functioning directly on NF-κB family members, selected poxviral NF-κB inhibitors may effectively suppress critical NF-κB-regulated responses without the need for the complementary action of other NF-κB inhibitors encoded by these viruses. An

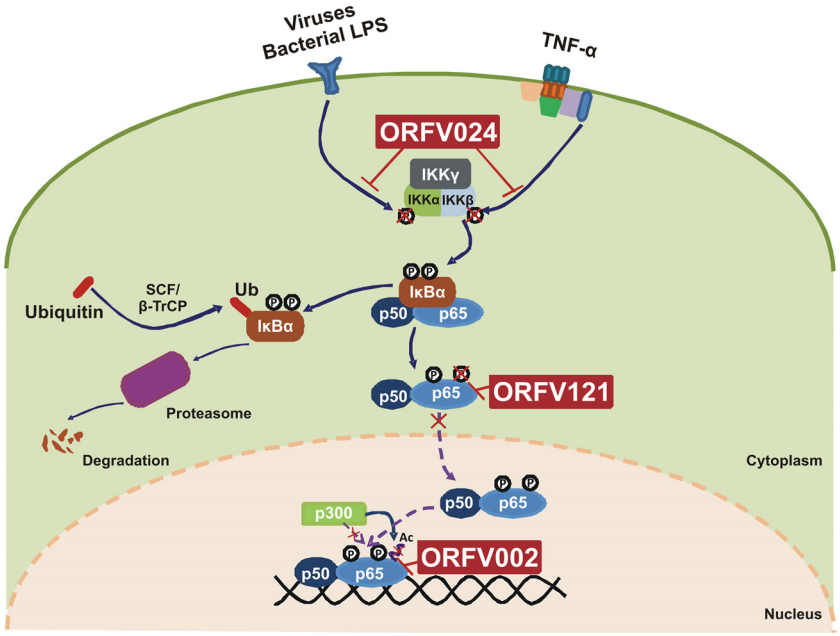

FIG. 9. NF-κB signaling pathway and its regulation by ORFV-encoded proteins ORFV024, ORFV121, and ORFV002. ORFV024 inhibits the phosphorylation of IκB kinases IKKα and IKKβ by targeting steps upstream of the IKK complex. ORFV121 binds to and inhibits the phosphorylation and nuclear translocation of NF-κB-p65. ORFV002 binds to and inhibits the p300-mediated acetylation of NF-κB-p65, likely by disrupting the association of p300 and NF-κB-p65.

exception here is ORFV-encoded ORFV002, which binds to and decreases the acetylation of NF-κB-p65 in the nucleus without significantly affecting virus virulence in the natural host (12). It would be interesting to determine if other poxviral encoded proteins that target NF-κB subunits (28, 29) have a similar effect on virus virulence and disease pathogenesis in natural hosts *in vivo*.

Poxviruses have evolved a striking variety of mechanisms to inhibit the NF-κB signaling pathway, targeting ligand-receptor interactions on the cell surface or intracellular cytoplasmic events of the pathway (28). Notably, while lacking homologues of most poxviral NF-κB inhibitors (an exception being *ORFV020*, a homologue of the VACV *E3L* gene), ORFV has evolved novel proteins to modulate NF-κB transactivating activity by targeting distinct aspects of the pathway, including both cytoplasmic and nuclear events (11, 12). ORFV-encoded ORFV024 functions in the cell cytoplasm upstream of the IKK complex, preventing the activation of IKK by inhibiting the phosphorylation of the IκB kinases IKKα and IKKβ (11). ORFV ORFV121 functions in the cell cytoplasm, immediately downstream of IκBα, by binding to and inhibiting the phosphorylation and nuclear translocation of NF-κB-p65, while ORFV-encoded ORFV002 functions in the cell nucleus, where it binds to and inhibits the acetylation of NF-κB-p65 (Fig. 9) (12). Given the complexity of the NF-κB signaling pathway and the broad spectrum of cellular processes regulated by this pathway, it is not surprising that ORFV, like other poxviruses, has evolved an array of mechanisms to interfere with NF-κB-regulated responses. Indeed, it is possible that ORFV encodes additional NF-κB inhibitors, either novel ones or those conserved in other chordopoxviruses, such as the ankyrin repeat-containing family of proteins (10, 47) to effectively suppress NF-κB-regulated host cell responses.

In summary, we have described a third novel NF-κB inhibitor encoded by ORFV. ORFV121 binds to NF-κB-p65 in the cell cytoplasm, suppressing its phosphorylation, nuclear translocation, and consequently transactivating activity. The deletion of *ORFV121* from the ORFV genome resulted in an attenuated disease phenotype in sheep, indicating that ORFV121 represents a *bona fide* virulence determinant for ORFV in the natural host.

ACKNOWLEDGMENTS

We thank J. Shisler (Department of Microbiology, University of Illinois), L.-F. Chen (Department of Biochemistry University of Illinois), T. Shors (Department of Biology and Microbiology, University of Wisconsin–Oshkosh), M. Varela and P. R. Murcia (Institute of Comparative Medicine, University of Glasgow Veterinary School, United Kingdom), D. Refojo (Max Planck Institute of Psychiatry, Munich, Germany), and G. McFadden (College of Medicine University of Florida) for providing plasmids used in this study, and we thank F. A. Osorio (Nebraska Center for Virology, University of Nebraska–Lincoln) for laboratory support.

REFERENCES

1. **Bartlett, N., J. A. Symons, D. C. Tscharke, and G. L. Smith.** 2002. The vaccinia virus N1L protein is an intracellular homodimer that promotes virulence. J. Gen. Virol. **83:**1965–1976.
2. **Bohuslav, J., L. F. Chen, H. Kwon, Y. Mu, and W. C. Greene.** 2004. p53 induces NF-kappaB activation by an IkappaB kinase-independent mechanism involving phosphorylation of p65 by ribosomal S6 kinase 1. J. Biol. Chem. **279:**26115–26125.
3. **Bowie, A., et al.** 2000. A46R and A52R from vaccinia virus are antagonists of host IL-1 and toll-like receptor signaling. Proc. Natl. Acad. Sci. U. S. A. **97:**10162–10167.
4. **Camus-Bouclainville, C., et al.** 2004. A virulence factor of myxoma virus colocalizes with NF-kappaB in the nucleus and interferes with inflammation. J. Virol. **78:**2510–2516.

5. **Chang, S. J., et al.** 2009. Poxvirus host range protein CP77 contains an F-box-like domain that is necessary to suppress NF-kappaB activation by tumor necrosis factor alpha but is independent of its host range function. J. Virol. **83:**4140–4152.
6. **Chen, L. F., and W. C. Greene.** 2004. Shaping the nuclear action of NF-kappaB. Nat. Rev. Mol. Cell Biol. **5:**392–401.
7. **Chen, L. F., et al.** 2005. NF-kappaB RelA phosphorylation regulates RelA acetylation. Mol. Cell Biol. **25:**7966–7975.
8. **Chen, R. A., G. Ryzhakov, S. Cooray, F. Randow, and G. L. Smith.** 2008. Inhibition of IkappaB kinase by vaccinia virus virulence factor B14. PLoS Pathog. **4:**e22.
9. **de la Concha-Bermejillo, A., J. Guo, Z. Zhang, and D. Waldron.** 2003. Severe persistent orf in young goats. J. Vet. Diagn. Investig. **15:**423–431.
10. **Delhon, G., et al.** 2004. Genomes of the parapoxviruses ORF virus and bovine papular stomatitis virus. J. Virol. **78:**168–177.
11. **Diel, D. G., G. Delhon, S. Luo, E. F. Flores, and D. L. Rock.** 2010. A novel inhibitor of the NF-kappaB signaling pathway encoded by the parapoxvirus orf virus. J. Virol. **84:**3962–3973.
12. **Diel, D. G., et al.** 2011. A nuclear inhibitor of NF-κB encoded by a poxvirus. J. Virol. **85:**264–275.
13. **DiPerna, G., et al.** 2004. Poxvirus protein N1L targets the I-kappaB kinase complex, inhibits signaling to NF-kappaB by the tumor necrosis factor superfamily of receptors, and inhibits NF-kappaB and IRF3 signaling by toll-like receptors. J. Biol. Chem. **279:**36570–36578.
14. **Dvoracek, B., and T. Shors.** 2003. Construction of a novel set of transfer vectors to study vaccinia virus replication and foreign gene expression. Plasmid **49:**9–17.
15. **Erickson, G. A., E. A. Carbrey, and G. A. Gustafson.** 1975. Generalized contagious ecthyma in a sheep rancher: diagnostic considerations. J. Am. Vet. Med. Assoc. **166:**262–263.
16. **Fleming, S. B., and A. A. Mercer.** 2007. Genus *Parapoxvirus*, p. 127–165. *In* A. A. Mercer, A. Schmidt, and O. Weber (ed.), Poxviruses. Birkhäuser, Basel, Switzerland.
17. **Gedey, R., X. L. Jin, O. Hinthong, and J. L. Shisler.** 2006. Poxviral regulation of the host NF-kappaB response: the vaccinia virus M2L protein inhibits induction of NF-kappaB activation via an ERK2 pathway in virus-infected human embryonic kidney cells. J. Virol. **80:**8676–8685.
18. **Guo, J., et al.** 2003. Characterization of a North American orf virus isolated from a goat with persistent, proliferative dermatitis. Virus Res. **93:**169–179.
19. **Haig, D. M., and C. J. McInnes.** 2002. Immunity and counter-immunity during infection with the parapoxvirus orf virus. Virus Res. **88:**3–16.
20. **Haig, D. M., and A. A. Mercer.** 1998. Ovine diseases. Orf. Vet. Res. **29:**311–326.
21. **Harte, M. T., et al.** 2003. The poxvirus protein A52R targets Toll-like receptor signaling complexes to suppress host defense. J. Exp. Med. **197:**343–351.
22. **Hautaniemi, M., et al.** 2010. The genome of pseudocowpoxvirus: comparison of a reindeer isolate and a reference strain. J. Gen. Virol. **91:**1560–1576.
23. **Jenkinson, D. M., P. E. McEwan, V. A. Moss, H. Y. Elder, and H. W. Reid.** 1990. Location and spread of orf virus antigen in infected ovine skin. Vet. Dermatol. **1:**189–195.
24. **Johnston, J. B., et al.** 2005. A poxvirus-encoded pyrin domain protein interacts with ASC-1 to inhibit host inflammatory and apoptotic responses to infection. Immunity **23:**587–598.
25. **Karin, M., and Y. Ben-Neriah.** 2000. Phosphorylation meets ubiquitination: the control of NF-kappaB activity. Annu. Rev. Immunol. **18:**621–663.
26. **Liu, B., et al.** 2008. IKKalpha is required to maintain skin homeostasis and prevent skin cancer. Cancer Cell **14:**212–225.
27. **McKeever, D. J., D. M. Jenkinson, G. Hutchison, and H. W. Reid.** 1988. Studies of the pathogenesis of orf virus infection in sheep. J. Comp. Pathol. **99:**317–328.
28. **Mohamed, M. R., and G. McFadden.** 2009. NFkappaB inhibitors: strategies from poxviruses. Cell Cycle **8:**3125–3132.
29. **Mohamed, M. R., et al.** 2009. Proteomic screening of variola virus reveals a unique NF-kappaB inhibitor that is highly conserved among pathogenic orthopoxviruses. Proc. Natl. Acad. Sci. U. S. A. **106:**9045–9050.
30. **Mohamed, M. R., et al.** 2009. Cowpox virus expresses a novel ankyrin repeat NF-kappaB inhibitor that controls inflammatory cell influx into virus-infected tissues and is critical for virus pathogenesis. J. Virol. **83:**9223–9236.
31. **Moss, B.** 2007. Poxviruses: the viruses and their replication, p. 2905–2946. *In* D. M. Knipe and P. M. Howley (ed.), Fields virology, 5th ed., vol. 2. Wolters Kluwer Health/Lippincott Williams & Wilkins, Philadelphia, PA.
32. **Mourtada, I., M. Le Tourneur, J. Chevrant-Breton, and F. Le Gall.** 2000. Human orf and erythema multiforme. Ann. Dermatol. Venereol. **127:**397–399.
33. **Murao, L. E., and J. L. Shisler.** 2005. The MCV MC159 protein inhibits late, but not early, events of TNF-alpha-induced NF-kappaB activation. Virology **340:**255–264.
34. **Myskiw, C., J. Arsenio, R. van Bruggen, Y. Deschambault, and J. Cao.** 2009. Vaccinia virus E3 suppresses expression of diverse cytokines through inhibition of the PKR, NF-kappaB, and IRF3 pathways. J. Virol. **83:**6757–6768.
35. **Ndikuwera, J., et al.** 1992. Chronic contagious ecthyma and caseous lymphadenitis in two Boer goats. Vet. Rec. **131:**584–585.
36. **Nestle, F. O., P. Di Meglio, J. Z. Qin, and B. J. Nickoloff.** 2009. Skin immune sentinels in health and disease. Nat. Rev. Immunol. **9:**679–691.
37. **Nettleton, P. F., J. A. Gilray, D. L. Yirrell, G. R. Scott, and H. W. Reid.** 1996. Natural transmission of orf virus from clinically normal ewes to orf-naive sheep. Vet. Rec. **139:**364–366.
38. **Nichols, D. B., and J. L. Shisler.** 2009. Poxvirus MC160 protein utilizes multiple mechanisms to inhibit NF-kappaB activation mediated via components of the tumor necrosis factor receptor 1 signal transduction pathway. J. Virol. **83:**3162–3174.
39. **Pasparakis, M.** 2009. Regulation of tissue homeostasis by NF-kappaB signalling: implications for inflammatory diseases. Nat. Rev. Immunol. **9:**778–788.
40. **Perkins, N. D.** 2006. Post-translational modifications regulating the activity and function of the nuclear factor kappa B pathway. Oncogene **25:**6717–6730.
41. **Perkins, N. D.** 2007. Integrating cell-signalling pathways with NF-kappaB and IKK function. Nat. Rev. Mol. Cell Biol. **8:**49–62.
42. **Rahman, M. M., M. R. Mohamed, M. Kim, S. Smallwood, and G. McFadden.** 2009. Co-regulation of NF-kappaB and inflammasome-mediated inflammatory responses by myxoma virus pyrin domain-containing protein M013. PLoS Pathog. **5:**e1000635.
43. **Sanchez, R. L., A. Hebert, H. Lucia, and J. Swedo.** 1985. Orf. A case report with histologic, electron microscopic, and immunoperoxidase studies. Arch. Pathol. Lab. Med. **109:**166–170.
44. **Scheidereit, C.** 2006. IkappaB kinase complexes: gateways to NF-kappaB activation and transcription. Oncogene **25:**6685–6705.
45. **Seitz, C. S., Q. Lin, H. Deng, and P. A. Khavari.** 1998. Alterations in NF-kappaB function in transgenic epithelial tissue demonstrate a growth inhibitory role for NF-kappaB. Proc. Natl. Acad. Sci. U. S. A. **95:**2307–2312.
46. **Shisler, J. L., and X. L. Jin.** 2004. The vaccinia virus K1L gene product inhibits host NF-kappaB activation by preventing IkappaBalpha degradation. J. Virol. **78:**3553–3560.
47. **Sonnberg, S., S. B. Fleming, and A. A. Mercer.** 2009. A truncated two-alpha-helix F-box present in poxvirus ankyrin-repeat proteins is sufficient for binding the SCF1 ubiquitin ligase complex. J. Gen. Virol. **90:**1224–1228.
48. **Stack, J., et al.** 2005. Vaccinia virus protein A46R targets multiple Toll-like-interleukin-1 receptor adaptors and contributes to virulence. J. Exp. Med. **201:**1007–1018.
49. **Vallabhapurapu, S., and M. Karin.** 2009. Regulation and function of NF-kappaB transcription factors in the immune system. Annu. Rev. Immunol. **27:**693–733.
50. **Wan, F., and M. J. Lenardo.** 2010. The nuclear signaling of NF-kappaB: current knowledge, new insights, and future perspectives. Cell Res. **20:**24–33.
51. **Weisfelner, M. E., and A. B. Gottlieb.** 2003. The role of apoptosis in human epidermal keratinocytes. J. Drugs Dermatol. **2:**385–391.
52. **Yirrell, D. L., H. W. Reid, M. Norval, G. Entrican, and H. R. Miller.** 1991. Response of efferent lymph and popliteal lymph node to epidermal infection of sheep with orf virus. Vet. Immunol. Immunopathol. **28:**219–235.